

Study of neutron dose equivalent at the HIRFL deep tumor therapy terminal

Jun-Kui Xu(徐俊奎)^{1,2;1)} You-Wu Su(苏有武)^{1;2)} Wu-Yuan Li(李武元)¹⁾ Wei-Wei Yan(严维伟)¹⁾
Zong-Qiang Li(李宗强)¹⁾ Wang Mao(毛旺)¹⁾ Cheng-Guo Pang(庞成果)²⁾ Chong Xu(徐翀)¹⁾

¹⁾ Institute of Modern Physics, Chinese Academy of Sciences, Lanzhou 730000, China

²⁾ School of Nuclear Science and Technology, Lanzhou University, Lanzhou 730000, China

Abstract: The secondary neutron fields at the deep tumor therapy terminal at HIRFL (Heavy Ion Research Facility in Lanzhou) were investigated. The distributions of neutron ambient dose equivalent were measured with a FHT762 Wendi-II neutron ambient dose equivalent meter as ^{12}C ions with energies of 165, 207, 270, and 350 MeV/u were bombarded on thick tissue-like targets. The thickness of targets used in the experiments was larger than the range of the carbon ions. The neutron spectra and dose equivalent were simulated by using FLUKA code, and the results agree well with the experimental data. The experiment results showed that the neutron dose produced by fragmentation reactions in tissue can be neglected in carbon-ion therapy, even considering their enhanced biological effectiveness. These results are also valuable for radiation protection, especially in the shielding design of high energy heavy ion medical machines.

Keywords: deep tumor therapy, neutron dose equivalent, radiation protection

PACS: 07.88.+y, 41.60.Ap **DOI:** 10.1088/1674-1137/41/6/068201

1 Introduction

Carbon ions are the most common particle in heavy ion tumor therapy, due to their physical and biological properties. The so-called “Bragg peak” of heavy ions makes them very suitable for radiotherapy. However, secondary particles caused by heavy ion reactions must be taken into account in the shielding design of heavy ion medical machines and personal dose assessment. Neutrons are the most abundant of all secondary particles and very important in safety evaluation for radiation protection. Furthermore, neutrons can affect a large area due to their strong penetrating power. That is to say, they can influence the whole body of the patient, including tumor and healthy tissue.

In recent years, there have been many studies on the secondary neutrons induced by mid-energy heavy ions and protons bombarding on thick targets. For example, Sunil et al. measured the neutron dose equivalent in low energy (about 7 MeV/u) heavy ion interactions with thick targets [1, 2]. In 2012, Nandy et al. measured the neutron dose equivalent distribution in carbon ion-induced reactions with Ti and Ag targets using proton recoil scintillator [3]. In view of radiation protection of patients, Haluk Yucel et al. measured the neutron dose

equivalent at a 18-MV medical linac [4] in 2015. Howell et al. measured neutron dose equivalents in craniospinal irradiation by a passively scattered proton system [5]. Saeed et al. calculated the ambient dose equivalent of fast neutrons by using the elemental composition of the human body and the conversion coefficient ICRP116 [6]. T. Kurosawa et al. performed a systematic experimental study on neutron yields, spectra and angular distributions of various ions on thick targets with a TOF method at HIMAC (Heavy Ion Medical Accelerator in Chiba), and compared their experiments with the HIC code calculation results [7, 8].

In our previous work, the secondary neutrons induced by heavy ions were also studied. G. Li et al. measured neutron yields from 50–100 MeV/u heavy ions hitting thick targets using the activation method at HIRFL IMP [9]. Neutron dose equivalent distributions have been measured at the superficial tumor treatment terminal of HIRFL. In that experiment, carbon ions were accelerated to 100 MeV/u by the separated-sector cyclotron (SSC) of HIRFL, and then delivered vertically down to a basement where the superficial tumor treatment terminal is located [10]. These studies are useful for radiation protection, including neutron shielding design, and also have significance in tumor therapy.

Received 12 July 2016, Revised 4 December 2016

1) E-mail: xujunkui@impcas.ac.cn

2) E-mail: suyowu@impcas.ac.cn

©2017 Chinese Physical Society and the Institute of High Energy Physics of the Chinese Academy of Sciences and the Institute of Modern Physics of the Chinese Academy of Sciences and IOP Publishing Ltd

The maximum energy of ^{12}C ions is 100 MeV/u when the ions are extracted from the SSC, which is not high enough for deep tumor therapy. However, HIRFL-CSR could be used to accelerate the carbon ions to higher energies (the maximum energy is 900 MeV/u) to study the deep tumor therapy. Figure 1 shows the layout of the HIRFL-CSR and the location of the deep tumor therapy terminal. In the present work, the neutron dose was measured at this deep tumor therapy terminal as carbon ions with specific energy of 165, 207, 270 and 350 MeV/u bombarded thick tissue-like targets. Then we calculated neutron dose distribution and energy spectra with FLUKA code. It is found that the measured neutron dose results are in good agreement with the calculated results.

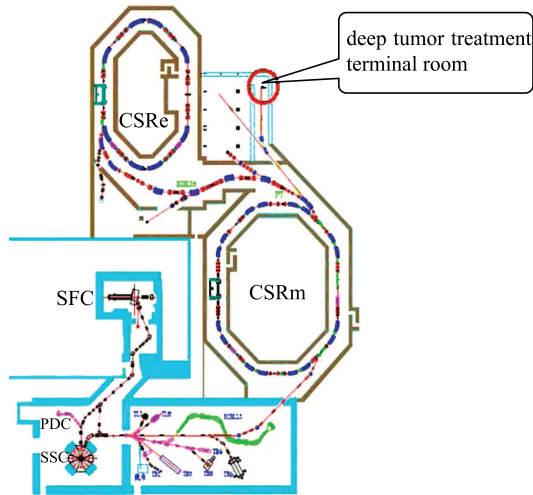


Fig. 1. (color online) Schematic diagram of the HIRFL-CSR.

2 Experimental apparatus

The experiment was carried out at the deep tumor therapy terminal of HIRFL-CSR. ^{12}C ions were accelerated to 80 MeV/u by SSC then injected into CSRm for accelerating to the energies needed. In this work, the carbon ion energies were chosen as 165, 207, 270 and 350 MeV/u. In order to measure the ion counts, the extracted ^{12}C ions first penetrated a parallel plate ionization chamber detector, filled with nitrogen gas at atmospheric pressure, which in this work was used to count the number of primary particle. Then the ions were delivered to the deep tumor therapy terminal. A tissue-like target thick enough to stop the ions was placed on the treatment bed. Table 1 lists the material composition of the target. The target was a superposition of several thin slices, whose cross section was 30 cm \times 30 cm. Table 1 shows the thickness of the tissue-like target used for different incident energy carbon ions.

For monitoring the produced neutrons a modified A-B rem-meter detector [11] was placed at the same height as the target (1.2 meters above the floor) in this experiment. Here, we call it the FHT672 Wendi II neutron ambient dose equivalent meter. It uses a large volume He-3 tube and can measure neutrons with energies ranging from thermal to 5 GeV. Calculations show that adding a heavy metal material layer to the rem-meter can increase the neutron response at high energies while keeping the response curve unchanged in the lower energy region [12–14]. It should be noted that there is an uncertainty in measuring the high energy neutron dose because of the lack of mono-energetic neutron sources for calibrating the detector. However, if the neutron spectra can be simulated it is possible to obtain the neutron dose by correcting the measured results with a standard A-B rem-meter.

Table 1. Material composition of the tissue-like target. The density is (1.043 ± 0.005) g/cm³.

component	proportion(%)
H	8.1
C	67.2
N	2.4
O	19.9
Cl	0.1
Ca	2.3

Table 2. The thickness of the tissue-like targets used for different carbon ion energies.

ion energy/(MeV/u)	target thickness/cm
165	8
207	12
270	18
350	26

In the measurements, when the number of accumulated counts in the parallel plate ionization chamber detector reaches 4×10^5 , the primary beam is automatically cut off, and the FHT672 Wendi-II neutron ambient dose equivalent meter stops recording the neutron dose equivalent. Then the Wendi-II detector is shifted to another observation position and the primary beam is extracted again. Using this method, neutron dose emitted from the target was measured at 0°, 30°, and 90° at different distances.

3 Monte Carlo simulation

A detailed description of the FLUKA code can be found in the previous paper [15]. In our simulation, a parallel ^{12}C beam was delivered to a tissue-like target with the same size and composition as used in the experiment (Tables 1 and 2). The size of the treatment room

filled with dry air is $4\text{ m} \times 5.6\text{ m} \times 8\text{ m}$. The simulation geometry only includes the shielding wall and the target; other accessories are neglected for a simplicity. The cross section diameter of the mono-energetic beam is 5 mm with Gaussian distribution. In the sampling process one carbon ion is extracted from the simulation source. The tissue-like target is bombarded by carbon ions with energies of 165, 207, 270 and 350 MeV/u. Here, the selected ion energies and the targets are consistent with the experimental parameters. In the process of simulation, the PHSICS card was used to select the specific class of transport problems, such as particle transport threshold, multiple scattering threshold, heavy fragment transport activated and so on. The USRBDX card was used to obtain the neutron energy spectra, and in the Monte Carlo simulation a set of detectors was placed at 1 meter from the injection point at different angles as shown in Fig. 2. The total histories in the simulation were from 10^9 to 8×10^9 depending on the projectile energies. The relative error of the calculation was less than 5%. The USRBIN card was chosen to obtain the neutron dose equivalent. FLUKA version 2011.2c was used in this work.

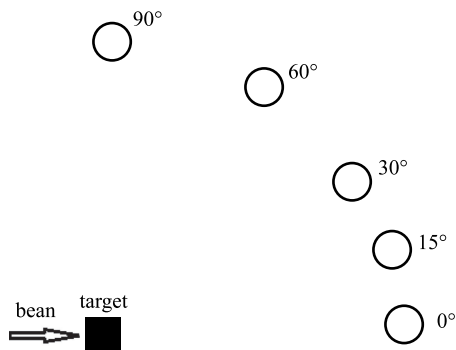


Fig. 2. The geometric arrangements for calculating the neutron energy spectra.

4 Results and discussion

Figure 3 shows the measured neutron ambient dose equivalent as a function of the distance from the target to the FHT672 Wendi-II detector. The solid squares represent the neutron dose equivalent induced by carbon ions with energy of 350 MeV/u, and the circles, up-triangles and down-triangles represents the doses by carbon ions with energies of 270, 207 and 165 MeV/u, respectively. The parallel plate ionization chamber was used as a counter. For carbon ion energies from 165 MeV/u to 400 MeV/u, one count of the ionization chamber represents about 900 to 1300 carbon ions. So the chamber will approximately make a response as 1100 carbon ions with an error of $\pm 18\%$ penetrating it. According to the calibration test report, the linear error of the FHT672 is from -9% to 11% and the angular dependence error

is about $\pm 20\%$. Therefore, the error of the data measured by FHT672 Wendi-II neutron meter is from -22% to 23% . The total uncertainty of the dose as shown in Fig. 3 is less than $\pm 30\%$.

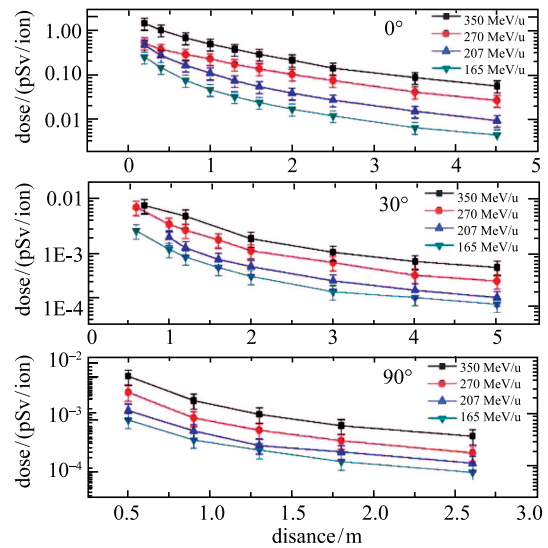


Fig. 3. (color online) The measured neutron dose equivalent as a function of the distance from the center of the targets to the FHT672 Wendi-II neutron meter for observation angles of 0° , 30° and 90° , respectively. Squares, circles, up-triangles and down-triangles represent carbon ions with energies of 350, 270, 207, and 165 MeV/u, respectively.

As can be seen from Fig. 3, the measured results show the following characteristics. (1) At the same position in the deep tumor terminal room, the neutron dose equivalent increases with the increase of the carbon ion energies. This is because the neutron yield produced by the fragmentation reaction increases with increasing carbon ion energy. (2) With the same incident energies of the carbon ions, the neutron dose equivalent decreases approximately exponentially with increasing distance from the dose meter to the tissue-like target center. Moreover, the decreasing shape becomes more approximately consistent at larger angles. (3) The neutron dose at 0° is about 100 times larger than the dose at 90° for the same incident energies. This can be explained by the neutron yields at small angles being larger than at large angles, and the cascade neutrons being the major part of the neutron yield, i.e., the neutron emission has a sharp forward peak. At large angles, the measured neutrons are mainly from the low energy evaporation mechanism.

In order to understand the cumulative amount of neutron dose equivalent in a simplified treatment process,

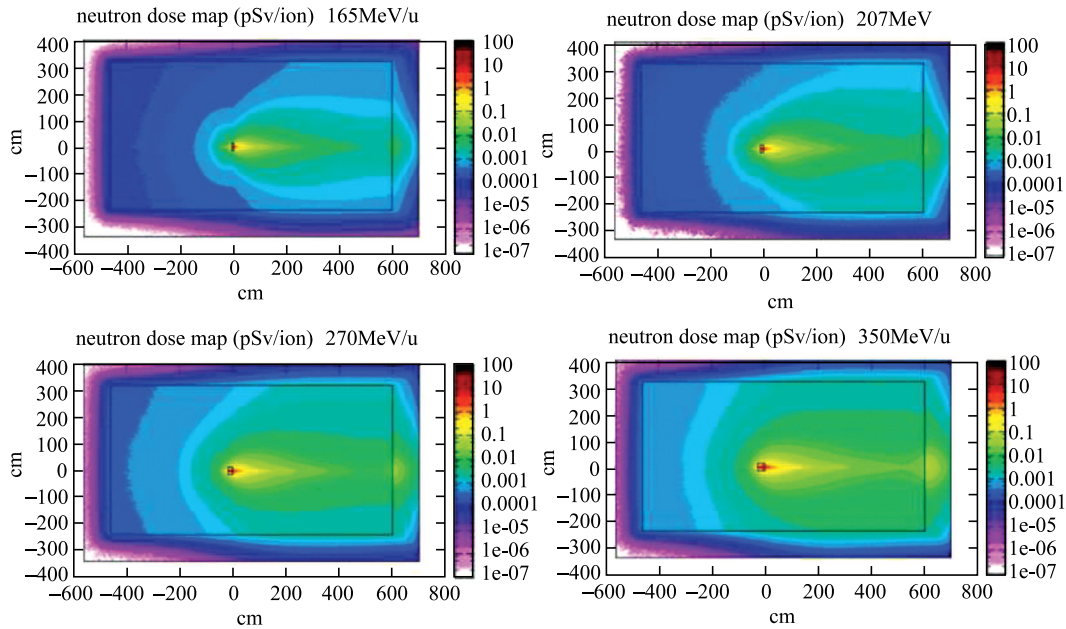


Fig. 4. (color online) The calculated neutron dose equivalent distributions induced by carbon ions with energies of 165, 207, 270 and 350 MeV/u, respectively.

we can make a qualitative estimate. The accumulated counts measured by the parallel plate ionization chamber in ordinary carbon ion therapy with energy of 350 MeV/u is about 1×10^7 . Therefore, the accumulated neutron dose equivalent at 20 cm from the target center at 0° is about 15 mSv. Based on this number, the neutron absorbed dose is estimated as a few mGy, which is a low level compared with the treatment dose in carbon ion therapy [16]. This indicates that the neutron dose produced by fragmentation reactions in tissue is small and even can be ignored, despite their enhanced biological effectiveness in radiotherapy.

The FLUKA simulated results of the neutron dose distribution are shown in Fig. 4. The top left represents the results induced by 165 MeV/u carbon ions, and the top right those from 207 MeV/u carbon ions. The bottom left represents the distribution from 270 MeV/u carbon ions, and the bottom right those from 350 MeV/u carbon ions. The simulated results exhibit the same tendency as the measured results, i.e., the neutron dose equivalent increases as the projectile energy increases, and the dose at 0° is much higher than at 90° . It should be noted that the neutron dose equivalent at 0° near the shielding wall increases with the increase of the incident energies. This result could be explained by the (n, xn) spallation reaction happening as the high energy neutrons bombard the concrete wall [17], and the neutron yield increasing as the carbon ion energies increase.

The neutron dose equivalent at 0° calculated with the FLUKA code is shown in Fig. 5 together with the experimental results. The solid symbols represent the mea-

sured data, and the lines represent the FLUKA simulations. The shapes of the simulated results agree well with the measured ones, but the absolute values are about 2.1 times those of the experimental data. In Fig. 5 the experimental data are shown with their absolute values. The discrepancy could have the following causes. Firstly, the detector itself cannot achieve the ideal requirement, namely its energy response to neutrons is not absolutely consistent with the human response. The second reason is related to the uncertainty of the primary ion counts. Finally, the differences may be from the program code itself.

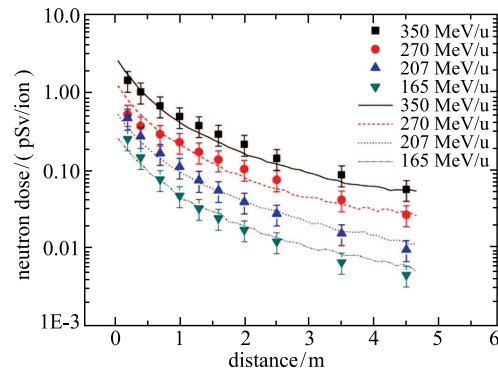


Fig. 5. (color online) The experimental and calculated neutron dose equivalent at 0° for different incident energies. The symbols represent the experiments: squares, circles, up-triangles and down-triangles represent carbon ions with energies of 350, 270, 207, 165 MeV/u, respectively. The lines represent the corresponding simulation results.

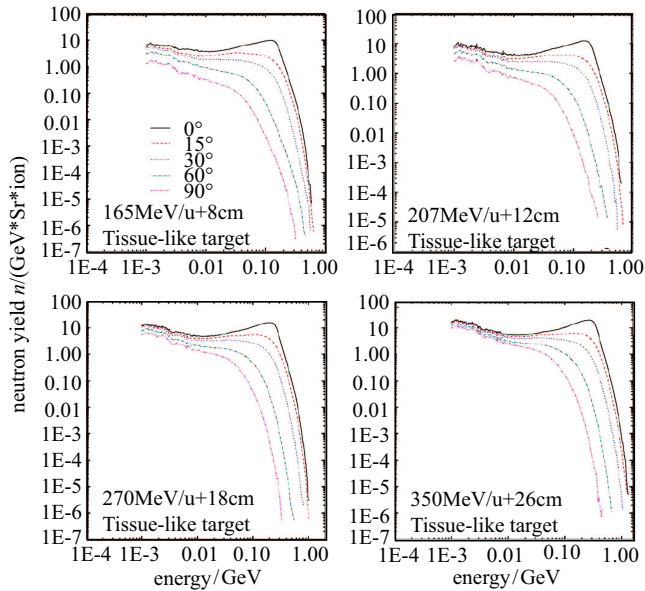


Fig. 6. (color online) The calculated neutron energy spectra of ^{12}C ions bombarding a tissue-like target.

In order to further interpret the measured neutron dose equivalent, the neutron energy spectra were also calculated with the FLUKA code for ^{12}C ions with energies of 165, 207, 270 and 350 MeV/u, respectively, bombarding a thick tissue-like target. The neutron dose can be calculated from the neutron spectra by using the flux to dose conversion factors ($H^*(10)$) of ICRP publication number 74 [18]. The calculated results are shown in Fig. 6. As can be seen from the figure, there is a broad peak at the high energy range in the forward direction, and the yield of high energy neutrons decreases swiftly as the angle is increased. This means that the measured

higher intensity neutrons at 0° as mentioned above are high energy neutrons, which are produced in the cascade (or pre-equilibration) process. It can also be seen that the neutrons below 10 MeV are approximately independent of the energies of the primary carbon ions and the ejection angles. This means that these neutrons are produced isotropically by the equilibrium (or evaporation) mechanism.

5 Conclusions

In this work, we measured the neutron dose distribution at the HIRFL deep tumor treatment terminal as 165, 207, 270 and 350 MeV/u ^{12}C ions, respectively, bombarded tissue-like targets. It was found that the neutron dose decreases approximately exponentially with the distance from the target to the tissue-like target, and the dose at 0° is about 100 times larger than that at 90° for the same distance. The experimental results indicate that the neutron dose equivalent produced by fragmentation reactions in tissue is small as compared with the treatment dose. We also calculated the neutron dose distribution by using FLUKA code. The results were in agreement with the experimental data except for a constant factor. The secondary neutron energy spectra were also calculated. The measurements and the simulations are valuable for radiation protection, especially in the shielding design of high energy heavy ion medical machines and personal dose assessment.

This work was performed under the direction of Prof. Xiao Guo-Qing and Prof. Zhao Hong-Wei, with the help of Dr. Li Qiang, Dr. Hu Zheng-Guo and other members of the medical group at IMP. Here, the authors would like to express their appreciation to all of them.

References

- 1 C. Sunil, A. Saxena, R. K. Choudhury et al, Nuclear Instruments and Methods in Physics Research A, **534**: 518–530 (2004)
- 2 C. Sunil, A. A. Shanbhag, M. Nandy et al, Radiation Measurements, **47**: 1035–1043 (2012)
- 3 M. Nandy, P. K. Sarkar, T. Sanami et al, Radiation Measurements, **45**: 1276–1280 (2012)
- 4 Haluk Yucl, Ibrahim Cobanbas, Asuman Kolbas et al, Nuclear Engineering and Technology, **48**(2): 525–532 (2016)
- 5 Rebecca M. Howell, Eric A. Burgett, Daniel Isaacs BS et al, International Journal of Radiation Oncology Biology Physics, **95**(1): 249–257 (2015)
- 6 A. Saeed, Sherif S. Nafee, Salem A. Shaheen et al, Applied Mathematics and Computation, **274**: 604–610 (2016)
- 7 T. Nakamura, the 4th International meetings of SATIF, **17-18**: 37–56 (1998)
- 8 T. Nakamura, N. Nakao, T. Kurosawa et al, Nuclear Science and Engineering, **132**(1): 30–57 (1999)
- 9 Guishegn Li, Tianmei Zhang, Zongwei Li et al, Nuclear Instruments and Methods in Physics Research A, **431**: 194–200 (1999)
- 10 Youwu Su, Zongqiang Li, Wuyuan Li et al, Chin. Phys. C, **34**(5): 548–550 (2010)
- 11 I. O. Andersson, J. A. Braun, *Proceedings of the IAEA Symposium on neutron dosimetry* (Vienna, 1963) **2**: 87–95 (1963)
- 12 C. Birattari, A. Ferrari, C. Nuccetelli et al. Nuclear Instruments and Methods in Physics Research A, **297**(1-2): 250–257 (1990)
- 13 V. Mares, A. V. Sannikov, H. Schraube, Nuclear Instruments and Methods in Physics Research A, **476**: 341–346 (2002)
- 14 C. Birattari, Adolfo Esposito, Alfredo Ferrari et al, Rad. Prot. Dosim., **76**(3): 135–148 (1998)
- 15 Junkui Xu, Youwu Su, Wuyuan Li et al, Chin. Phys. C, **40**(1): 018201-1–018201-4 (2016)
- 16 D. Schardt, T. Elsasser, D. Schulz-Ertner. Reviews of Modern Physics, **82**(1): 383–425 (2010)
- 17 Dazhao Ding, *Neutron physics*, The first edition (Beijing China:Atomic Energy Press, 2001), p.243 (in Chinese) (2001)
- 18 International Commission on Radiological Protection, Conversion coefficients for use in radiological protection against external radiation, first edition (Beijing China:Atomic Energy Press, 1998)P.94 (in Chinese) (1998)